5. Initiation of Cleavage Microcracks in Polycrystalline Iron and Steel

G. T. HAHN, B. L. AVERBACH, W. S. OWEN,* MORRIS COHEN

Department of Metallurgy
Massachusetts Institute of Technology

ABSTRACT

The results of tensile tests carried out at low temperatures are presented here for two steels and a vacuum-melted ferrite in several conditions of grain size. Plastic deformation and twinning associated with the microcracks have been studied in considerable detail. These findings, correlated with observations of microcracks, define the role of crack initiation in the over-all fracture process. Quantitative data are reported on the incidence and morphology of microcrack formation as a function of grain size, temperature, strain, and strain rate. These results are compared with the predictions of current theories.

Introduction

Several current theories dealing with the atomic mechanism of cleavage fracture in b.c.c. materials postulate that a crack is initiated by the pile-up of dislocations against an obstacle. The theories are usually tested through their predictions on the relation of fracture stress to grain size and temperature. However, the resulting agreements may be more apparent than real because of the large scatter in fracture data; moreover, it is often impossible to distinguish among the various theories on the basis of the restricted information available. On the other hand, the dislocation theories usually consider in some detail the sequence of events leading to the initiation of cleavage, and in certain instances it appears that the basic concepts may be critically tested by observations of the processes

* Now at the University of Liverpool, Liverpool, England.

that attend the very early indications of cleavage. Such observations have now been made for a variation of materials, grain size, temperature, and strain rate. The findings are examined in the light of current theory.

Dislocation Models for Cleavage

Zener [1] suggested that cleavage is preceded by slip; that is, a pile-up of dislocations against an obstacle, such as a grain boundary, can produce sufficient stress concentration to initiate a crack. The Zener model indicates that the crack will form in a plane approximately normal to the operative slip plane. However, Bullough [2] has proposed that the pile-up will generate a crack within the plane of slip. Cottrell [3] reconsidered the problems associated with a simple dislocation pile-up and postulated that two active intersecting (110) slip planes in b.c.c. materials generate a cleavage microcrack on the common (100) plane. Finally, Orowan [4] has suggested that a crack may be produced in the plane of slip by a polygonized array of dislocations.

TABLE 1. Theoretical Expressions* for the Stress to Initiate Cleavage Fracture, Based on Different Dislocation Models

		Equation Number
Zener model according to Stroh: [5]	$\sigma_s = \frac{4.4\gamma}{nb}$	(1)
Cottrell model: [3]	$\sigma_n = \frac{2.3\gamma}{n'b}$	(2)
Bullough model according to Gilman: [7]	$\sigma_n = \frac{5.3\gamma}{nb}$	(3)
Orowan model according to Stroh: [6]	$\sigma_n = \frac{2.7\gamma}{nb}$ †	(4)

σ_s = applied shear stress in excess of stress required to move dislocations
σ_n = normal stress
n = number of dislocations piled up against a grain boundary
n' = number of dislocations that enter crack
b = Burgers vector
γ = effective surface energy term
L = length of the vertical array of dislocations
l = length of the dislocation pile-up
G = shear modulus

* Constants involving π and Poisson's ratio ($\frac{1}{3}$ for iron and steel) have been evaluated.

† The actual expression derived by Stroh is: $\sigma_s\sigma_n = 1.3\gamma G/L$. It is assumed that $L = l$ and that $\sigma_s l = Gbn$.[8]

These models have been treated quantitatively by Stroh,[5,6] Cottrell,[3] and Gilman.[7] Expressions for the stress to initiate cleavage are summarized in Table 1. It is generally assumed that a crack, successfully initiated within a grain, will continue to grow and cause fracture. The effective surface energy term γ, which appears in each of the expressions (Table 1), may be regarded as a disposable parameter. For this reason, experimental fracture-stress values cannot be used to test the theory. Furthermore, inasmuch as the expressions derived for the different dislocation models have very similar forms, the relationships do not provide a good means for distinguishing among the various models.

A number of difficulties with the pile-up models of crack initiation remain to be reconciled. One is associated with the cleavage microcracks, a grain diameter in length or larger, that have been reported by Low [9] and by Owen, Averbach, and Cohen.[10] The Stroh [5] treatment assumes that the first cleavage crack to grow beyond atomic dimensions continues to propagate and cause fracture. Since there is no provision for stopping cracks, the Stroh theory implies that no microcracks should be observed. Alternatively, in the Cottrell theory, the length of the largest stable microcrack is given by the following equation (this relationship is implied in the Cottrell derivation):

$$C = \frac{2G\gamma}{\pi(1-\nu)\sigma_n^2} \tag{5}$$

where G is the shear modulus (8×10^{12} dynes/cm^2), γ is the effective surface energy, ν is Poisson's ratio ($\frac{1}{3}$), and σ_n is the normal stress. Calculations of the critical crack size are summarized in Table 2 for fracture-stress values reported by Cottrell [3] and Low [9] and for a surface energy term $\gamma = 18{,}000$ ergs/cm^2 consistent with the Cottrell theory.[3] These results illustrate that the sizes of microcracks predicted by the Cottrell model are an order of magnitude smaller than the microcracks actually observed (1 to 2 grain diameters in length). Thus, it appears that neither the Stroh nor Cottrell theory accounts satisfactorily for the microcrack observations.

TABLE 2. Critical Microcrack Size According to Cottrell Theory [3]

Fracture Stress (dynes/cm^2)	Corresponding Grain Diameter (mm)	Calculated Critical Microcrack Length (mm)
7.2×10^9 (Ref. 3)	0.025	0.0026
5.3×10^9 (Ref. 9)	0.11	0.0049

Another difficulty is that high stresses generated by the pile-up can also nucleate slip in adjoining regions. Such deformation will relieve the stress concentration at the pile-up and inhibit crack formation. Consequently, some means of restraining plastic flow in the vicinity of the pile-up must be provided. Stroh [5] suggests that interstitial locking of dislocations furnishes the necessary restraints during the initial stages of plastic deformation. Hence, the occurrence of cleavage fracture should be restricted to the early stages of plastic deformation. Alternatively, Cottrell [3] proposes that the intersecting slip mechanism provides a more effective stress concentration than the Zener-Stroh model and concludes that cleavage can occur during yielding, or after discontinuous yielding is complete, or even as a consequence of preyield microstrain. This argument is open to question, however, because the stresses required to initiate cleavage by the Cottrell [3] and Zener-Stroh [5] mechanisms are essentially the same if comparable assumptions are made in the derivations of the relevant equations. (Compare Eqs. 10 and 13 of Cottrell [3] with Eqs. B1 and B6 of Stroh.[5])

Some Recent Experimental Work

Tensile data on two steels and a vacuum-melted ferrite (obtained on 0.252-in. diameter tensile bars tested at a constant applied strain rate of 0.02/min) have been obtained [11,12] for various grain sizes at temperatures ranging from the ambient down to −250°C. These data are summarized in Figs. 1 to 5. The composition of the materials and the treatments used are listed in Table 3.

The fracture phenomena exhibited by mild steel, for example in Fig. 1, may be divided into several temperature regions. In region *A*, the specimen undergoes necking and breaks with a characteristic cup-and-cone fracture; cleavage is not observed. In region *B*, necking still occurs, but the fracture starts in the necked region with a fibrous crack at the center of the specimen and converts to cleavage in an annular rim before rupture is complete. The fracture appearance, which is expressed in terms of the percentage of fibrous area, thus indicates the size of the initiating fibrous crack prior to cleavage. It is seen (from Fig. 1, for instance) that the critical size of fibrous crack to initiate the cleavage fracture decreases as the temperature is lowered in this region. The fracture transition T_f is analogous to the 50% fibrous appearance convention in Charpy specimens. At the boundary between regions *B* and *C*, the fracture stress and the reduction in area fall abruptly. This behavior defines the ductility transition temperature T_d.

TABLE 3. Compositions, Heat-Treatments, and Grain-Size Data

Material	Wt % C	Mn	Other					
E	0.22	0.36	P	0.016	S	0.031	Si	0.002
			Cu	0.17	Ni	0.13	Cr	0.08
			V	0.005	Mo	0.025	Al	0.009
			Sn	0.012	As	0.001	O	0.006
M	0.16	1.30	P	0.10	S	0.024	Si	0.024
F2	0.039	—	Si	0.01	Cu	0.005	Cr	0.01
			V	0.003	Mo	0.01	Al	0.003
			Sn	0.005	O	0.0011	N	0.002

Material	Heat-Treatment	Ferrite Grain Size	
		ASTM	*d* (mm)
E (coarse)	1250°C, 24 hr, AC 1250°C, 1 hr, FC	4	0.106
E (fine)	1250°C, 24 hr, AC 900°C, 1 hr, FC	7	0.041
M	As Received	7	0.034
F2 (very coarse)	1250°C, 4 hr, FC	0	0.409
F2 (coarse)	920°C, 30 min, FC	4	0.113

AC = air-cooled
FC = furnace-cooled

Microcracks are observed at the lower end of region *B* and in region *C*. The frequency of microcrack occurrence is designated as the percentage of ferrite grains containing microcracks. These data are obtained from observations on the cylindrical surfaces of tensile bars. The gage sections of the bars are electropolished prior to testing; the bars are strained and then systematically examined under the microscope. Most of the microcracks observed are about the length of a ferrite grain, and typical examples are shown in Figs. 6 and 7. These microcracks are not confined to the surface of the test specimens; machining away successive layers of the gage section and electropolishing reveals microcracks in the interior as well.

Below T_d the fracture is completely cleavage and is initiated by cleavage microcracks. The frequency of microcracks rises with decreasing temperature in region *C*, and in the case of coarse-grained ferrite (Fig. 4)

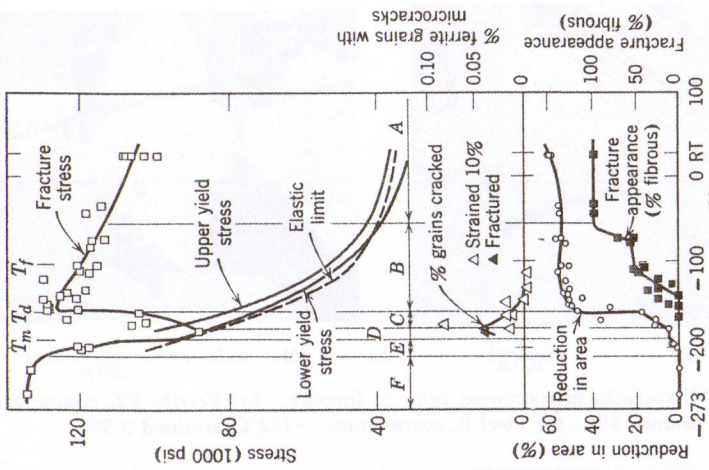

Fig. 1. Summary of tensile properties, fracture appearance, and microcrack data for coarse-grained Project Steel E. (d = 0.106 mm.)

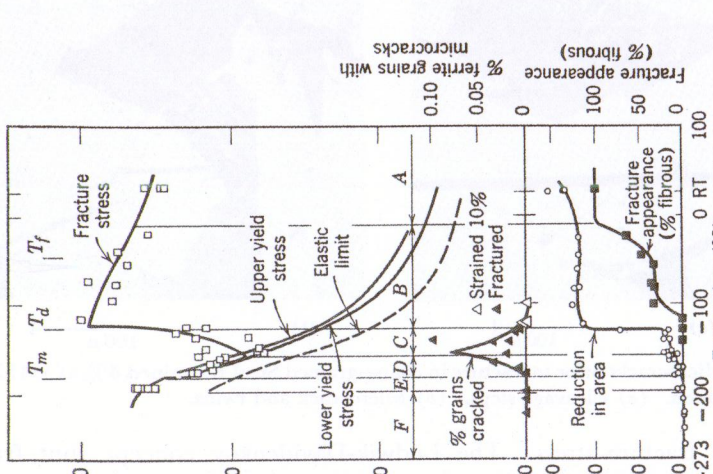

Fig. 2. Summary of tensile properties, fracture appearance, and microcrack data for fine-grained Project Steel E. (d = 0.041 mm.)

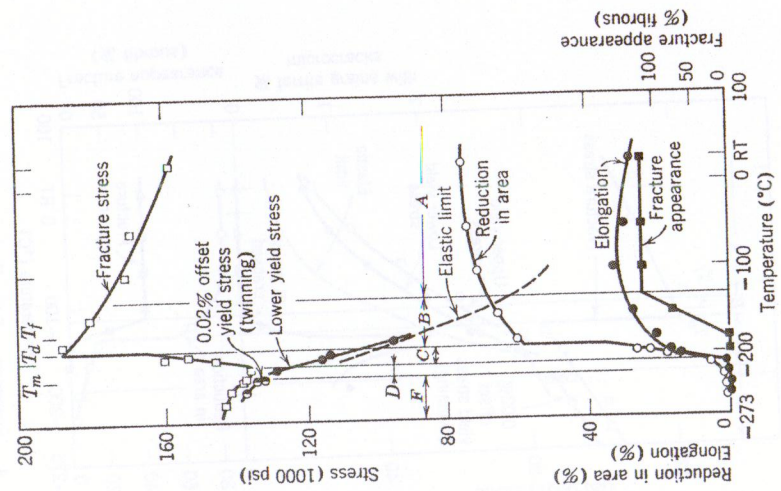

Fig. 3. Summary of tensile properties and fracture appearance of Steel M. (d = 0.034 mm.)

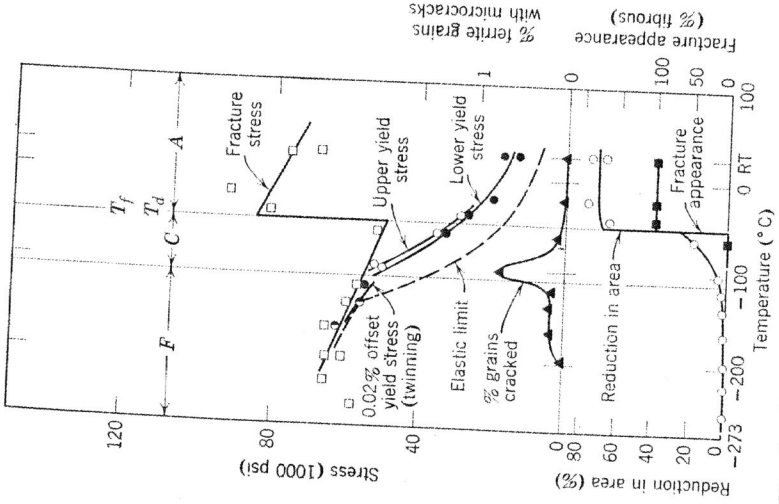

Fig. 5. Summary of tensile properties of very coarse-grained Ferrite F2. (d = 0.409 mm.)

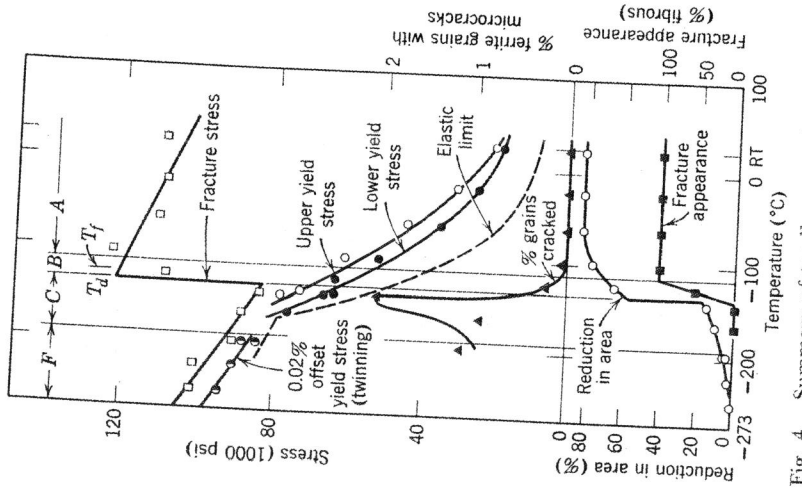

Fig. 4. Summary of tensile properties of coarse-grained Ferrite F2. (d = 0.113 mm.)

as many as 2% of the grains may be cracked. Nevertheless, the samples are not entirely brittle in this range. Immediately below the transition temperature T_d, for example, the elongation before fracture is from 10% to 20%, and there is a considerable difference between the yield stress

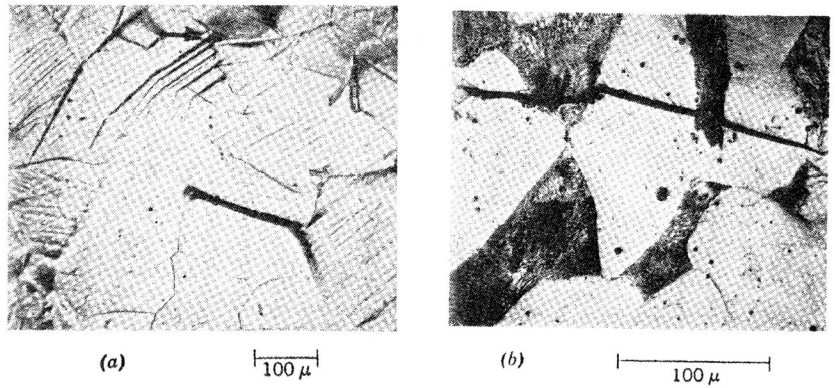

Fig. 6. Microcracks in specimens prior to fracture. (*a*) Ferrite F2, coarse grain, −140°C, strained 8%. (*b*) Steel E, coarse grain, −152°C, strained 3.5%.

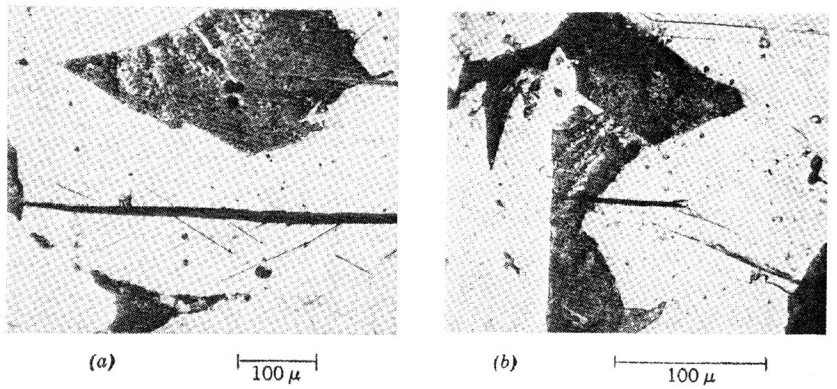

Fig. 7. Microcracks prior to fracture in coarse-grained Steel E strained 4% at −152°C and unloaded. (*a*) Cleavage steps. (*b*) Microcrack and twins.

and the fracture stress. The Ludwik-Davidenkov concept that fracture precedes yielding below the transition temperature is inconsistent with these findings.

The crack frequency in region B and in portions of region C is shown after 10% total elongation, that is, prior to necking and prior to fracture. At lower temperatures, microcrack data were obtained on fractured specimens, but the observations were confined to locations well removed from the main break.

In region D, the yield and fracture stresses are almost identical, but yielding is always observed prior to fracture. The fracture occurs at the lower yield stress. Microcracks are found in this temperature region, but only in areas of discontinuous strain, the latter being easily distinguished on the electropolished surface. The number of microcracks observed decreases as the temperature is lowered.

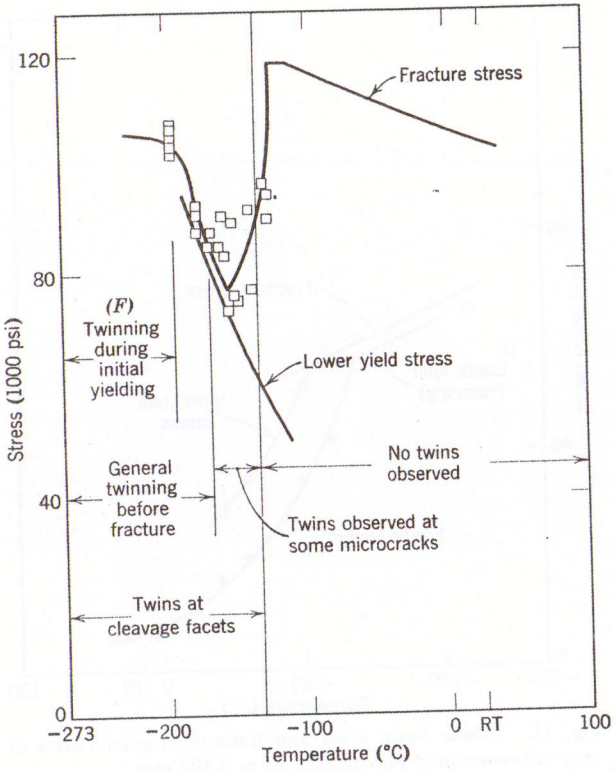

Fig. 8. Observations of twin formation in coarse-grained Steel E. (d = 0.106 mm.)

In region E, cleavage fracture occurs abruptly; the drop-in-load characteristic of yielding is not observed. Fracture stress values scatter about the extrapolated upper yield stress curve. It appears that the behavior in region E is an extension of D, and that cleavage fracture takes place in the very first location to undergo discontinuous yielding. Microcracks are not found in region E, presumably because the first one propagates to failure. The borderline between regions D and E is defined as the microcrack transition temperature T_m. This is the temperature at which propagation to failure occurs at the onset of gross yielding, and it corresponds to the criterion of brittleness defined by Cottrell.[3] Below T_m, fracture occurs at the upper yield stress rather than at the lower yield stress, because the tensile machine cannot unload rapidly enough.

In region F (Figs. 2 to 5), samples break abruptly, with the fracture stress values falling below extrapolations of the upper and lower yield stress curves. This region has often been identified with completely brittle

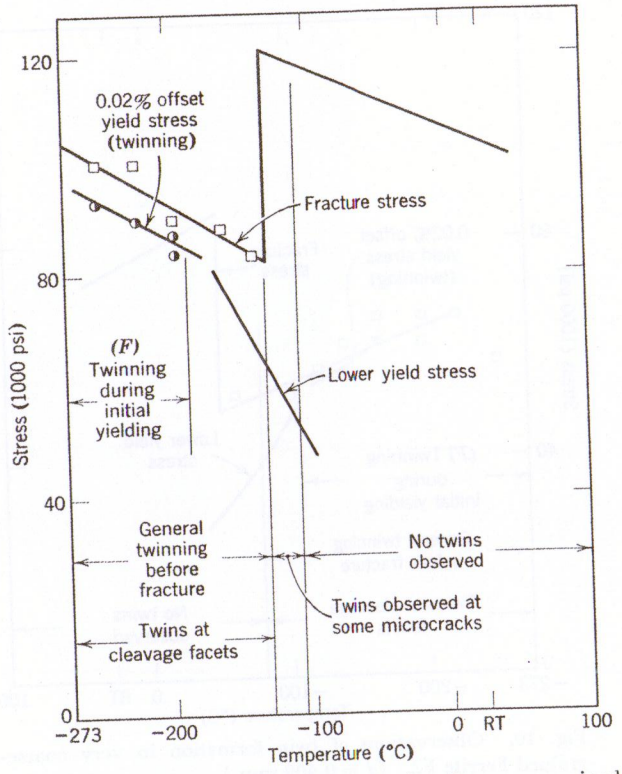

Fig. 9. Observations of twin formation in coarse-grained Ferrite F2. (d = 0.113 mm.)

fracture, that is, cleavage fracture without prior plastic deformation. However, the results of this study show that cleavage fracture in this range is associated with mechanical twinning. Twins actually begin to form in these materials at considerably higher temperatures after prior yielding; the extent of twinning and its influence on mechanical behavior increase as the test temperature is lowered.

The highest temperature at which twins are observed is in the general vicinity of T_d (Figs. 8 to 10). Here twins occur at the fracture as rectilinear markings on cleavage facets or at isolated microcracks. (These

markings have been described in some detail by Berry.[13]) However, as shown in Figs. 8 to 10, the onset of twinning does not, as a rule, coincide with T_d or with the appearance of microcracks. The indications are that twinning in the regions B and C is caused by the high stresses near cleavage cracks and that twinning here is not *responsible* for cleavage fracture. At somewhat lower temperatures, twins are no longer confined to the fracture but form throughout the sample before the rupture is complete. At temperatures close to region F, samples of Steel M and Ferrite F2 begin to twin before the upper yield point is reached. Twinning, accompanied by audible clicks, produces a serrated stress-strain curve, and the abrupt upper yield point is gradually suppressed as the testing temperature is decreased. In region F, the stress for the onset of deformation (yielding by twinning) exhibits an entirely different temperature dependence from that of the yield stress at higher temperatures. Essentially the same behavior has been described by Erickson and Low.[14]

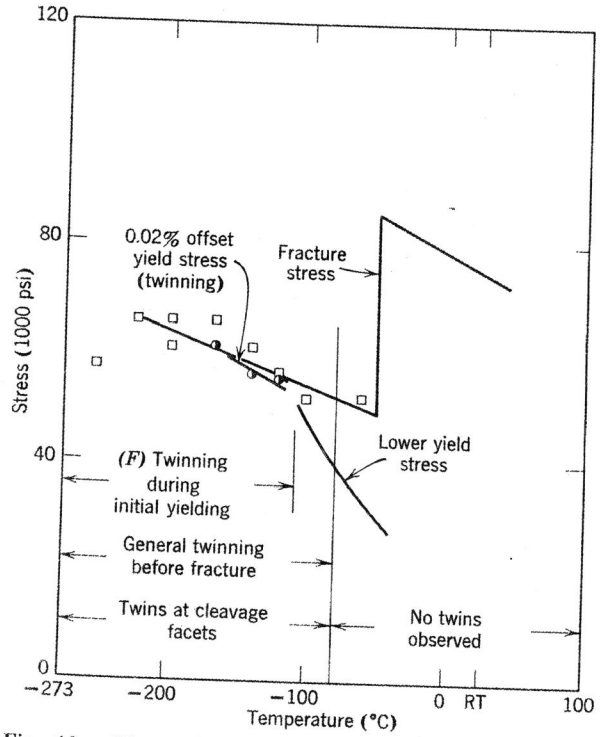

Fig. 10. Observations of twin formation in very coarse-grained Ferrite F2. (d = 0.409 mm.)

In region F, twin formation becomes a dominant factor in the cleavage fracture. The role of twin formation is probably best shown in coarse-grained ferrite samples (Fig. 4) where there is sufficient twinning to allow the measurement of a 0.02% offset stress prior to failure. It should be noted that the fracture stress in region F exhibits the same temperature dependence as the stress for twinning. At the lowest temperatures, stress-strain curves obtained for the very coarse-grained ferrite samples do not give evidence of deformation prior to fracture. However, the results of sensitive elastic limit measurements * presented in Fig. 11 demonstrate that cleavage fracture is preceded by discrete bursts of deformation of about 0.005% to 0.05% strain. The deformation is accompanied by audible clicks, and is identified as twinning. Here again, the fracture stress exhibits the same temperature dependence as the stress for the onset of twinning.

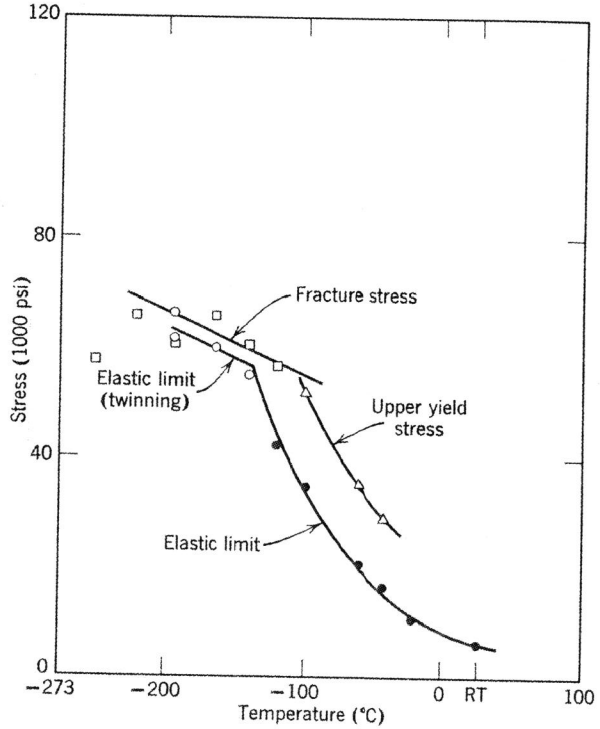

Fig. 11. Elastic limit, yield and fracture characteristics of very coarse-grained Ferrite F2. (d = 0.409 mm.)

* Elastic limit measurements were carried out by unloading from successively higher stresses and observing the first plastic strain (2×10^{-6}) discernible by means of an electrical resistance strain gage mounted on the specimen gage section. The stress required to produce a permanent set of 2×10^{-6} is defined as the elastic limit.

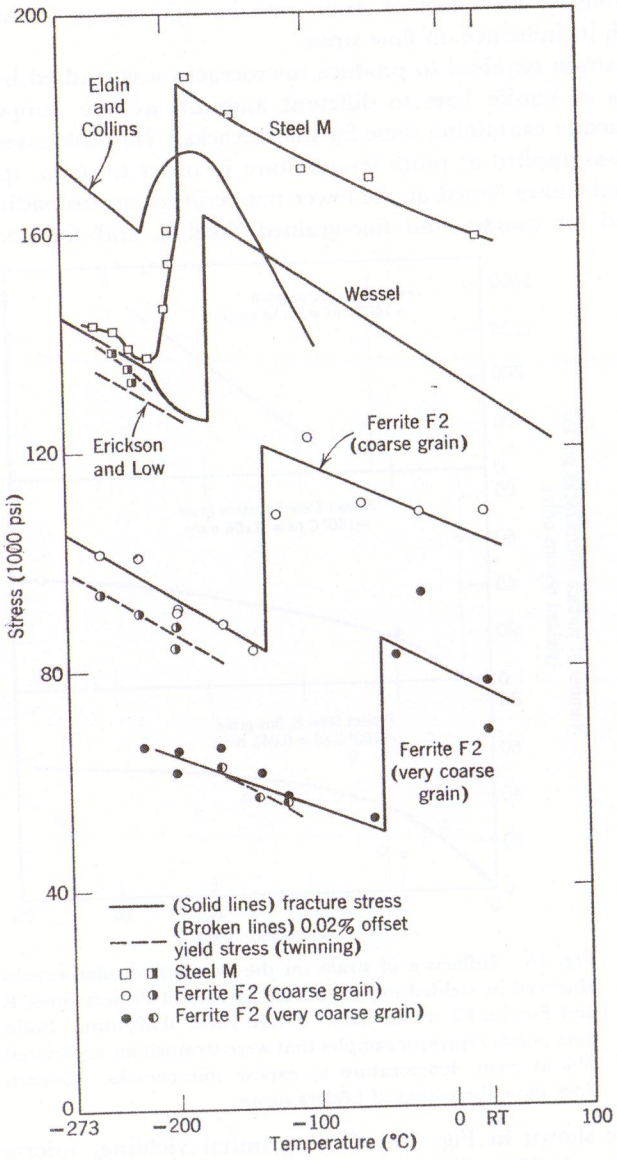

Fig. 12. Summary of twinning and fracture data of present investigation and of previous studies by Eldin and Collins,[15] Wessel,[16] and Erickson and Low.[14]

Some of the results of this study and previous work are summarized in Fig. 12. Similarities in the cleavage fracture behavior in region *F* are evident. In each case, the fracture stress parallels the stress for twinning. These findings indicate that twins initiate cleavage in region *F*, thereby performing the function attributed to slip in regions *C*, *D*, and *E*. Similar conclusions have recently been reached by Biggs and Pratt [17] from studies of iron single crystals at low temperatures.

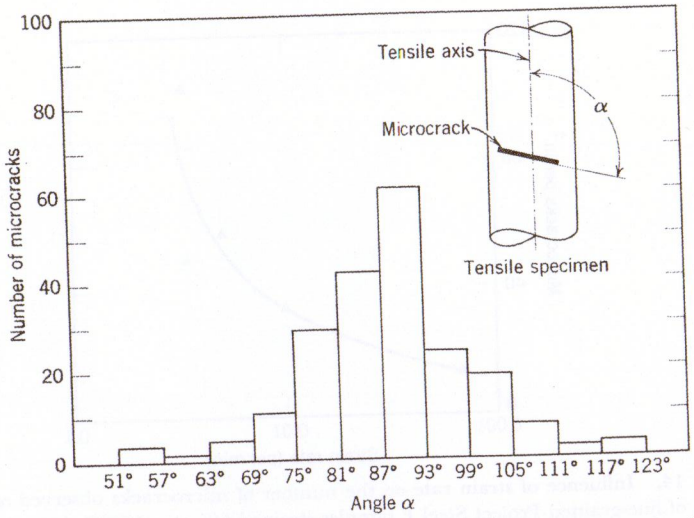

Fig. 13. Orientation of microcracks on the surface of coarse-grained Ferrite F2, strained 8% at −140°C, and unloaded.

Figures 1 and 2 show the several temperature regions in a coarse-grained and a fine-grained steel of the same composition. Corresponding data for the manganese steel are given in Fig. 3. The trend in fracture behavior is shifted to lower temperatures for the latter steel, twin-induced cleavages in region *F* occurring before the region *E* is observed. Twinning assumes an even more important role in the behavior of the coarse and very coarse-grained ferrite (Figs. 4 and 5). In these instances, twinning intervenes at even higher temperatures, and the phenomena associated with regions *D* and *E* are suppressed.

Measurements of the orientation of microcrack traces on the surface of a ferrite sample are presented in Fig. 13. Although orientations 40° on either side of the normal to the tensile axis are observed, 85% of the traces are oriented within 15° of a plane perpendicular to the tensile axis. It may be concluded that microcracks tend to form in a plane normal to the tensile axis.

The relation of microcrack formation to strain rate is shown in Fig. 14. These data, together with results obtained at different temperatures and constant strain rate, are plotted in Fig. 15 as a function of the lower yield stress measured in these tests. It appears that changes in the lower yield stress (used here as a measure of the level of stress) that are achieved by varying the strain rate have about the same effect on the number of microcracks as the changes produced by varying the test temperature.

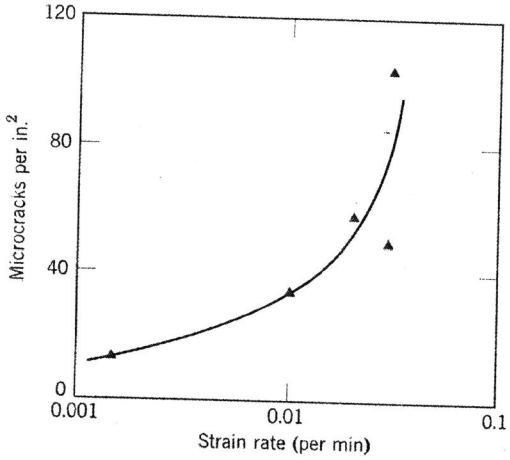

Fig. 14. Influence of strain rate on the number of microcracks observed on the surface of fine-grained Project Steel E samples strained 6% at −160°C. (d = 0.041 mm.)

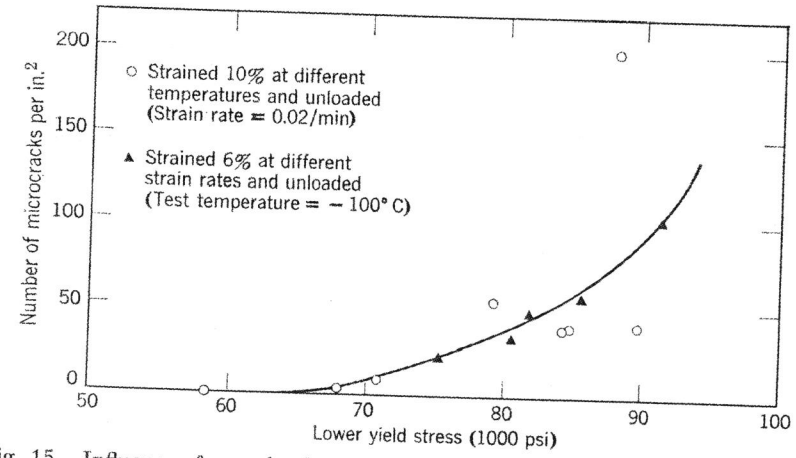

Fig. 15. Influence of stress level on the number of microcracks observed on the surface of fine-grained Project Steel E. (d = 0.041 mm.)

Undoubtedly, the effect of strain rate on microcrack formation comes through its influence on flow stress.

The strain required to produce microcracks was studied by deforming a series of tensile bars to different amounts at one temperature and subsequently examining these for microcracks. In some cases, additional strain was applied at room temperature in order to open up any cracks that might have closed at the lower temperature on unloading. Results obtained for coarse- and fine-grained Steel E and for coarse-grained

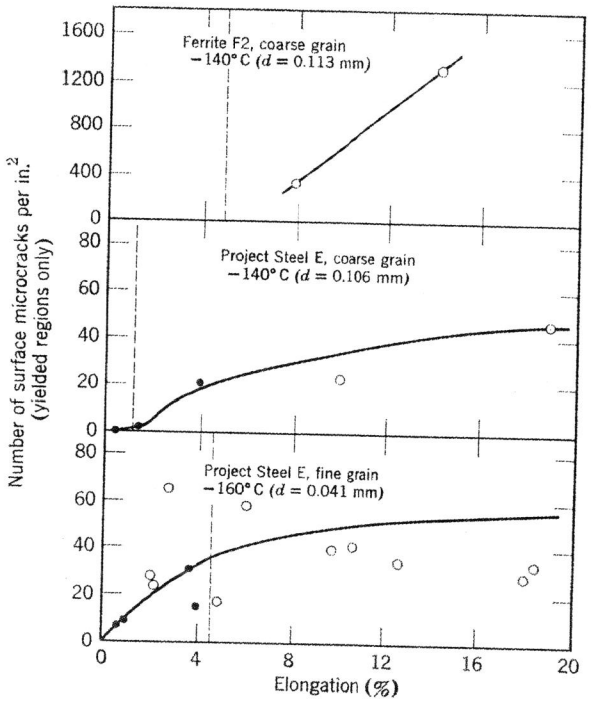

Fig. 16. Influence of strain on the number of microcracks observed in yielded regions on the surface of Project Steel E and Ferrite F2 tensile bars. Strain rate: 0.02/min. Solid data points represent samples that were strained an additional 5% at room temperature to expose microcracks. Broken lines show the extent of Lüders strain.

ferrite are shown in Fig. 16. During initial yielding, microcracks are observed in the fine-grained Steel E samples only in deformed regions *behind* the Lüders front, confirming previous observations on long, thin, flat specimens.[10] The microcrack densities quoted in Fig. 16 refer only to the yielded regions. Thus, the results for fine-grained samples indicate that the microcrack density behind the Lüders front continues to increase

while the discontinuous yielding propagates through the rest of the specimen. Therefore, the formation of microcracks, at least in this case, is not attributable to the initial yielding at the Lüders front; other processes occurring after the front has passed must be involved. In the coarse-grained samples, microcracks form only *after* the discontinuous yielding is complete. This is also suggested by the results obtained from the ferrite. Accordingly, the three sets of data in Fig. 16 are in agreement on the point that microcrack formation in the yielded regions or Lüders bands is not associated with the Lüders front.

Initiation and Propagation of Cleavage Fracture

Both Stroh [5] and Cottrell [3] have defined two stages in the process of cleavage fracture. The formation of a crack nucleus of atomic dimensions is regarded as *initiation;* the extension of this crack to critical dimensions (that is, $\sim\frac{1}{10}$ the grain diameter or smaller [5]) is termed *growth.* It is assumed that the crack, after attaining the critical size, will continue to grow, causing catastrophic cleavage fracture. The results of the present study demonstrate that large numbers of tiny cleavages are initiated subsequent to yielding in regions *B*, *C*, and *D*; these cleavages propagate to form microcracks, but do not result in fracture. Hence, the assumption that crack growth (as defined above) necessarily causes ultimate fracture does not appear valid. For the purposes of this discussion, the conditions for crack *initiation* are those which satisfy the requirements for both the initiation and the growth stages already described, that is, the conditions that lead to the formation of a crack which is critical with respect to the host grain. On the other hand, the conditions for crack *propagation* are those that satisfy the requirements for catastrophic cleavage fracture. On the basis of this and previous studies, it must be concluded that a cleavage crack that attains a size critical with respect to the host grain is not, at the same time, critical with respect to the over-all aggregate. In other words, the conditions for crack initiation do not necessarily satisfy the requirements for crack propagation. This implies that initiation and propagation are separate processes.

Models for cleavage initiation have been reviewed in the second section. Hypothetically, propagation may occur by one of the following processes. A growing microcrack may penetrate an adjoining grain and continue to propagate. The conditions for this type of propagation are prescribed by the Griffith-Orowan equation:

$$\sigma_n = \left(\frac{1.4\,E\gamma}{C}\right)^{1/2} \tag{6}$$

where σ_n is the normal stress, E is Young's modulus, γ the effective surface energy, and C the crack length. If the microcrack fails to penetrate further and stops at the grain boundary, propagation may then take place by the subsequent initiation of cracks in neighboring grains as a consequence of the stress concentration produced by the first unsuccessful cleavage. Since the applied stress alone satisfies the requirements for initiation in the first grain, the additional stress existing after the first crack is formed should produce additional cleavages in rapid succession until the Griffith-Orowan conditions for propagation are satisfied. Ultimate fracture should then occur shortly after the initiation of the first crack and before many other microcracks are formed. Because large numbers of microcracks are stable despite the action of the applied stress, it must be concluded that propagation by means of such reinitiation is difficult and that certain requirements for crack initiation apart from stress are not satisfied in the great majority of the grains. This requirement does not appear to be controlled by grain orientation, since there is considerable latitude in the orientations displayed by the microcracks (Fig. 13).

Another mechanism of propagation involves the possible connecting-up of random microcracks. Such cracks, if sufficiently numerous, could eventually be linked by ductile fracture of the bridging material. This could produce a large effective crack capable of propagating according to the Griffith-Orowan criterion. In the present investigation, microcracks are observed in no more than 2% of the grains, and therefore this mechanism seems unlikely.

In the temperature ranges *B*, *C*, and *D*, microcracks are initiated only in parts of the sample that have undergone yielding. In the ferrite specimens, microcracks may also be observed in region *F* after the onset of twinning (region *E* is absent). Although no microcracks are found in Steel E in regions *E* and *F*, the evidence cited in the previous section suggests that deformation (either slip or twinning) also precedes cleavage initiation in this temperature range. Plastic deformation appears to be a basic requirement for cleavage initiation in the materials studied.

The following processes are therefore prerequisites for cleavage fracture:

1. Plastic deformation.
2. Crack initiation.
3. Crack propagation.

In regions *B*, *C*, and *D* (and in parts of region *F* for the ferrite), microcracks are initiated after the onset of deformation but do not propagate. Consequently, propagation must be more difficult than initiation, the requirements for fracture being prescribed by the conditions for propagation. In regions *E* and *F* of Steel E, both initiation and propagation

follow immediately after slip or twinning. In this case, the conditions for yielding determine the occurrence of fracture.

Interpretation of Microcrack Studies

Evidence cited in the third section that cleavage is preceded by plastic deformation, whether slip or twinning, supports the view that dislocation arrays not present in annealed materials are important in crack initiation. The exact role of twinning is not clear. Stresses associated with twins may initiate cleavage directly. Twins may also act indirectly by nucleating slip [18] or by providing barriers to slip.[17] Since microcracks and cleavage fracture can occur entirely in the absence of twinning (Figs. 8, 9, and 10), twinning cannot be regarded as the exclusive mechanism for cleavage.

These studies have shown that microcracks are initiated after discontinuous yielding is locally complete and are not a direct consequence of the Lüders strain itself. Since dislocations are manifestly unpinned after initial yielding, dislocation locking is not an essential feature of cleavage fracture. Thus, the view advanced by Stroh [5] that the restraining of potential slip sources is accomplished by interstitial locking of dislocations does not seem realistic. The formation of microcracks appears to involve creep deformation behind the Lüders front [10] or subsequent deformation in the strain-hardening range. Moreover, the results presented in Fig. 16 indicate that microcracks do not form at the Lüders front despite a wide variation in the extent of the discontinuous deformation. This would suggest that the failure of cracks to form here is not related to a minimum strain requirement but must be attributed to some special characteristic within the Lüders strain.

One difference between the dislocation models is the postulated orientation of the initiated cleavage cracks. The Zener-Stroh, Bullough-Gilman, and Orowan-Stroh treatments predict that microcracks should tend to form at an angle of 55° to 60° to the tensile axis. On the other hand, the Cottrell mechanism tends to initiate cracks in a plane normal to the tensile axis. In view of the orientations plotted in Fig. 13, it appears that only the Cottrell model is consistent with orientations observed.

The stresses associated with the formation of microcracks furnish a means of testing the theory of cleavage *initiation*. Values of γ calculated for the Cottrell model (Eq. 2, Table 1) from data on Steel E and Ferrite F2 are listed in Table 4. It is assumed that cleavage is initiated at the yield stress and at the highest temperatures at which microcracks are observed. Under these conditions, the requirements for cleavage initiation are just satisfied. The value of n is calculated from the expression

TABLE 4. Effective Surface-Energy Values Calculated for Fine- and Coarse-Grained Steel E, and Coarse- and Very Coarse-Grained Ferrite F2, According to the Cottrell [3] Theory for Crack Initiation

	Steel E		Ferrite F2	
Grain Diameter (mm)	0.04	0.10	0.11	0.41
Normal Stress for Crack Initiation (dynes/cm²)	4.8×10^9 (−140°C)	3.6×10^9 (−120°C)	3.3×10^9 (−100°C)	1.6×10^9 (−20°C)
Effective Surface-Energy Term γ (ergs/cm²)	1.5×10^4	2.0×10^4	1.8×10^4	1.6×10^4

derived by Eshelby, Frank, and Nabarro,[8] assuming that σ_s is half the maximum shear stress, which in turn is half the normal stress. (This assumption is introduced to correct for the friction stress.) Since cleavage is initiated in the interior of the grain, the value of γ should be independent of grain size. The calculations show that γ is relatively constant over the wide range of grain sizes considered, a result that is in good agreement with the Cottrell theory. Inasmuch as the forms of the expressions developed for the other models are similar, this agreement extends to other treatments as well.

Values of the effective surface energy term γ consistent with the *propagation* of microcracks to ultimate cleavage (according to the Griffith-Orowan Eq. 6) are summarized in Table 5. The calculations are based on cleavage fracture-stress values immediately below the ductility transition temperature T_d. A crack size equal to the grain diameter is assumed. The values obtained are of the order of 10^5 ergs/cm², which is an order of magnitude larger than the effective surface energy for microcrack *initiation*. Since the term γ is a direct measure of the resistance to cleavage, this result expresses in quantitative terms the conclusion drawn in an earlier section that cleavage propagation is more difficult than initiation

TABLE 5. Effective Surface-Energy Values Calculated for Fine- and Coarse-Grained Steel E, and Coarse- and Very Coarse-Grained Ferrite F2, According to the Griffith-Orowan Theory for Crack Propagation

	Steel E		Ferrite F2	
Grain Diameter (mm)	0.04	0.10	0.11	0.41
Normal Stress for Crack Propagation, i.e., Fracture Stress (dynes/cm²)	7.8×10^9 (−160°C)	6.6×10^9 (−130°C)	5.7×10^9 (−140°C)	3.6×10^9 (−60°C)
Effective Surface-Energy Term γ (ergs/cm²)	0.9×10^5	1.5×10^5	1.3×10^5	1.9×10^5

and that the resistance to cleavage increases when the microcrack reaches a length commensurate with the grain size. This change in resistance may be associated with accommodations that attend the growth of the crack across grain boundaries, and grain boundaries may be regarded as barriers to cleavage.

At a temperature just above T_d, microcracks are also present prior to fracture, and the fracture is virtually all cleavage. Yet the fracture stress is significantly higher than at a temperature immediately below T_d. This abrupt alteration in fracture stress may be related to the change in extent of plastic deformation prior to fracture, that is, 45 to 65% vs. 10 to 20% reduction in area. Apparently, the large deformation that sets in above T_d enhances the resistance to crack propagation by further increasing the effective surface energy.

General Summary

The classical Griffith-Orowan treatment of brittle fracture describes the conditions for the propagation of cleavage fracture from pre-existing cracks. These cracks are drawn from the reservoir of flaws thought to be present in materials; no mechanism for initiation of the pre-existing cracks is provided. One difficulty with this approach is that the crack size consistent with the known strengths of some materials is unrealistic.[19] The dislocation models described in an earlier section overcome this difficulty but impose another requirement that some deformation precede fracture. Consequently, observations that cleavage fracture occurs prior to yielding at stresses below the level of the lower yield stress (as found in region *F*) have, in the past, been interpreted as evidence that pre-existing flaws are responsible for cleavage fracture. The results of this study show that quasi-brittle fracture below the lower yield stress merely reflects a change in the dominant mechanism of deformation from slip to twinning. Hence, these findings support current dislocation concepts of cleavage *initiation*. Calculations based on the stresses to produce microcracks in the materials studied here indicate that the available theoretical expressions satisfactorily describe the grain-size dependence of crack initiation. However, only the Cottrell model furnishes an explanation for the observed orientations of microcracks. On the other hand, the fact that many microcracks larger than the critical size predicted by the dislocation models are formed without inducing fracture demonstrates that the present treatments do not describe the conditions for cleavage propagation to fracture. The difficulty seems to arise from the circumstance that grain boundaries act as effective barriers to impede microcrack growth from one grain to the next.

Inasmuch as the formation of microcracks is restricted to a very small fraction of the grains despite substantial increases in stress (that is, in the vicinity of microcracks), the local stress cannot be the only factor playing an important part in the process of initiation. Another factor is considered to be the blocking of slip that would otherwise relieve the stress at dislocation pile-ups. Stroh [5] originally proposed that dislocation locking by interstitial atoms provides the necessary restraints during initial yielding. However, the present results show that crack initiation

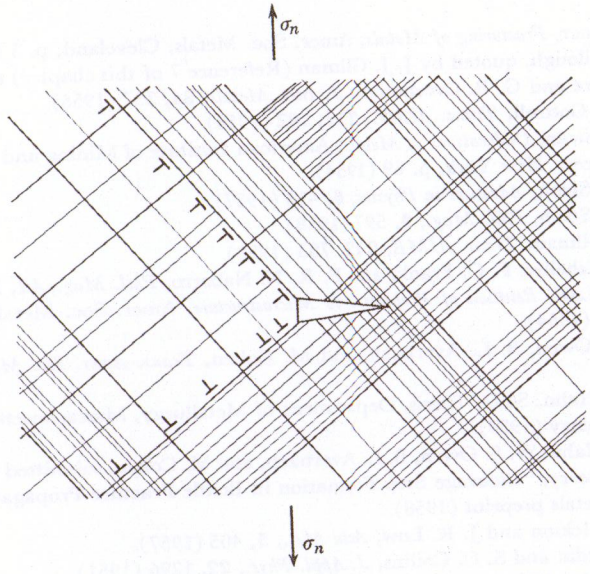

Fig. 17. Dislocation pile-up forming a microcrack in a region of heterogeneous deformation.

occurs, in fact, *after* discontinuous yielding, when dislocations are ostensibly unlocked. Dislocation locking, therefore, does not seem to be the answer. Since cleavage fracture is initiated in a region that has suffered Lüders strain or twinning, then local heterogeneous deformation, slip bands, or twins may provide some measure of constraint. As illustrated in Fig. 17, the stress concentration may occur by blockage of dislocations in regions that are so heterogeneously deformed that dislocation motion in them is extremely difficult. In general, it appears that the dislocation theories in this respect are still incomplete.

ACKNOWLEDGMENT

This research is part of a program at the Massachusetts Institute of Technology, sponsored by the Ship Structure Committee and under the advisory guidance of the Committee on Ship Steel of the National Academy of Sciences-National Research Council.

REFERENCES

1. C. Zener, *Fracturing of Metals*, Amer. Soc. Metals, Cleveland, p. 3 (1948).
2. R. Bullough, quoted by J. J. Gilman (Reference 7 of this chapter) and by A. Deruyttere and G. B. Greenough, *J. Inst. Metals*, **84**, 337 (1956).
3. A. H. Cottrell, *Trans. AIME*, **212**, 192 (1958).
4. E. Orowan, *Dislocations in Metals*, American Institute of Mining and Metallurgical Engineers, New York, p. 69 (1954).
5. A. N. Stroh, *Advances in Physics*, **6**, 418 (1957).
6. A. N. Stroh, *Phil. Mag.*, **3**, 597 (1958).
7. J. J. Gilman, *Trans. AIME*, **212**, 783 (1958).
8. J. D. Eshelby, F. C. Frank, and F. R. N. Nabarro, *Phil. Mag.*, **42**, 351 (1951).
9. J. R. Low, *Relation of Properties to Microstructure*, Amer. Soc. Metals, Cleveland, p. 163 (1954).
10. W. S. Owen, B. L. Averbach, and M. Cohen, *Trans. Amer. Soc. Metals*, **50**, 634 (1958).
11. G. T. Hahn, Sc.D. Thesis, Department of Metallurgy, Massachusetts Institute of Technology (1959).
12. G. T. Hahn, W. S. Owen, B. L. Averbach, and M. Cohen, submitted to *Welding J.*
13. J. M. Berry, "Cleavage Step Formation in Brittle Fracture Propagation," Amer. Soc. Metals preprint (1958).
14. J. S. Erickson and J. R. Low, *Acta Met.*, **5**, 405 (1957).
15. A. S. Eldin and S. C. Collins, *J. Appl. Phys.*, **22**, 1296 (1951).
16. E. T. Wessel, *Proc. ASTM*, **56**, 540 (1956).
17. W. D. Biggs and P. L. Pratt, *Acta. Met.*, **6**, 694 (1958).
18. W. H. Bruckner, *Welding J.*, **30**, 459s (1951).
19. E. Orowan, *Repts. Progr. in Phys.*, **12**, 185 (1949).

DISCUSSION

J. R. Low, Jr., *General Electric Research Laboratory*. The authors, in discussing yielding and fracture of iron at 78°K and below, make the suggestion that twinning may initiate microcracks and, by implication, total fracture in their materials. I would like to report the results of some metallographic work that shows that microcracks can in fact be initiated by twinning.

Two materials were examined, a low-carbon fine-grained iron and single crystals of 3% Si-Fe. Polished specimens of these materials were strained

to produce twinning without complete fracture; the low-carbon iron was strained at 20°K and the silicon iron at 78°K.

The polished surface of the fine-grained iron was then replicated by pressing a thin film of cellulose acetate, moistened with acetone, against the surface and dry stripping after the solvent had evaporated. Carbon was evaporated onto this negative plastic replica, and the plastic was then dissolved to obtain a carbon replica that could be examined in the electron microscope. Figures D.1 and D.2 are typical examples

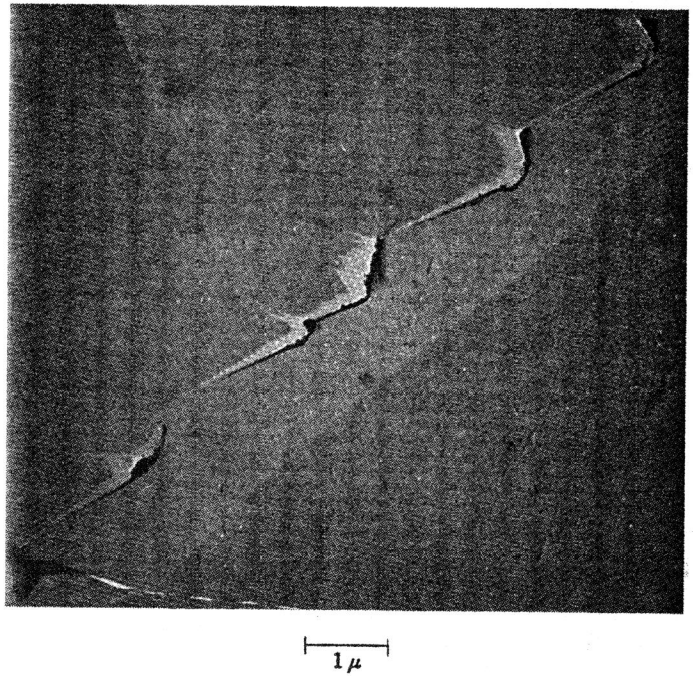

Fig. D.1. Microcracks at the twin-matrix interface.

of the types of microcracks observed. The dark protrusions represent cracks at the twin-matrix interface that have been filled by the impressed plastic. These cracks appear to form at the twin-matrix interface only where this interface becomes irregular during growth of the twin. Cracks are not observed on the smooth side of the twin, even though both interfaces move during growth. Cracks such as these have been observed for twins formed at all temperatures between 20° and 125°K. Above 125°K, twins are not observed in tension testing of this material.

Twin-interface cracks may also be revealed by lightly electropolishing the surface of a specimen after deformation. This effect, shown in Fig. D.3, also shows a matrix cleavage crack apparently originating from

a twin-interface crack, suggesting that total fracture may be nucleated by this mechanism. Figure D.3 was obtained from the surface of a single crystal of 3% Si-Fe deformed by bending at 78°F. Since the crystal orientation was known, it was possible to index the apparent cleavage crack using the trace of the twin as a (112) trace. The straight crack at an angle to the twin in Fig. D.3 is at the correct angle to be a cleavage crack on a (100) plane.

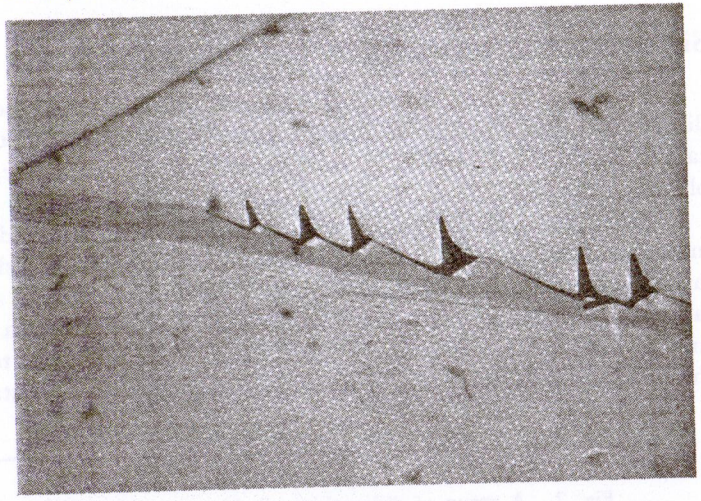

Fig. D.2. Microcracks at the twin-matrix interface.

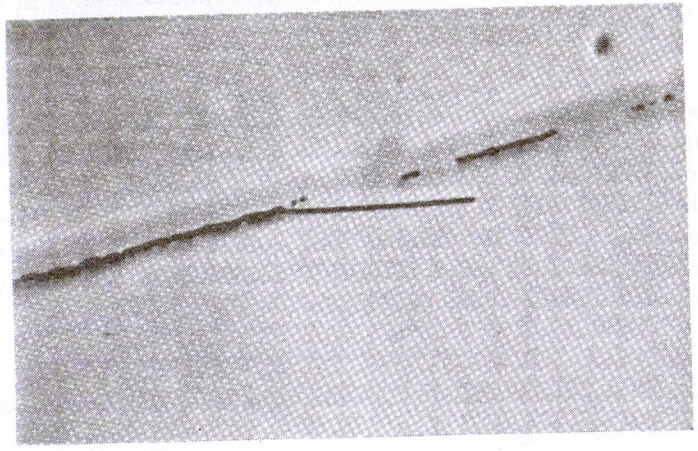

Fig. D.3. Matrix cleavage crack apparently originating from a twin-interface crack.